Title

Two serine residues in Pseudomonas syringae effector HopZ1a are required for acetyltransferase activity and association with the host co-factor.

Journal

The New phytologist, 208(4)

ISSN

1469-8137

Authors

Ma, Ka-Wai
Jiang, Shushu
Hawara, Eva
et al.

Publication Date

2015-12-01

DOI

10.1111/nph.13528

Peer reviewed

HHS Public Access

Author manuscript

New Phytol. Author manuscript; available in PMC 2016 February 26.

Published in final edited form as:

New Phytol. 2015 December ; 208(4): 1157–1168. doi:10.1111/nph.13528.

Two serine residues in *Pseudomonas syringae* effector HopZ1a are required for acetyltransferase activity and association with the host co-factor

Ka-Wai Ma[1,2,*], **Shushu Jiang**[1,2,*], **Eva Hawara**[1], **DongHyuk Lee**[3], **Songqin Pan**[2], **Gitta Coaker**[3], **Jikui Song**[4], and **Wenbo Ma**[1,2]

[1]Department of Plant Pathology and Microbiology, University of California, Riverside, CA 92521, USA

[2]Center for Plant Cell Biology, University of California, Riverside, CA 92521, USA

[3]Department of Plant Pathology, University of California, Davis, CA 95616, USA

[4]Department of Biochemistry, University of California, Riverside, CA 92521, USA

Summary

- Gram-negative bacteria inject type III secreted effectors (T3SEs) into host cells to manipulate the immune response. The YopJ family effector HopZ1a produced by the plant pathogen *Pseudomonas syringae* possesses acetyltransferase activity and acetylates plant proteins to facilitate infection.
- Using mass spectrometry, we identified a threonine residue, T346, as the main autoacetylation site of HopZ1a. Two neighboring serine residues, S349 and S351, are required for the acetyltransferase activity of HopZ1a *in vitro* and are indispensable for the virulence function of HopZ1a in *Arabidopsis thaliana*.
- Using proton nuclear magnetic resonance (NMR), we observed a conformational change of HopZ1a in the presence of inositol hexakisphosphate (IP6), which acts as a eukaryotic co-factor and significantly enhances the acetyltransferase activity of several YopJ family effectors. S349 and S351 are required for IP6-binding-mediated conformational change of HopZ1a.
- S349 and S351 are located in a conserved region in the C-terminal domain of YopJ family effectors. Mutations of the corresponding serine(s) in two other effectors, HopZ3 of *P. syringae* and PopP2 of *Ralstonia solanacerum*, also abolished their acetyltransferase activity. These results suggest that, in addition to the highly conserved catalytic residues, YopJ family effectors also require conserved serine(s) in the C-terminal domain for their enzymatic activity.

Author for correspondence: Wenbo Ma, Tel: +1 951 827 4349, wenboma@ucr.edu.

*These authors contributed equally to this work.

Supporting Information

Additional supporting information may be found in the online version of this article.

Please note: Wiley Blackwell are not responsible for the content or functionality of any supporting information supplied by the authors. Any queries (other than missing material) should be directed to the *New Phytologist* Central Office.

Keywords

acetyltransferase; *Arabidopsis thaliana*; bacterial virulence; inositol hexakisphosphate (IP6); *Pseudomonas syringae*; stomatal aperture; YopJ family type III effectors

Introduction

Plant innate immunity is divided into two branches (Jones & Dangl, 2006; Spoel & Dong, 2012). The first branch is based on the activation of pattern-triggered immunity (PTI) upon recognition of evolutionarily conserved microbial signatures called microbe- or pathogen-associated molecular patterns (MAMPs or PAMPs) by pattern recognition receptors (PRRs) located at the plasma membrane (Bohm *et al.*, 2014; Zipfel, 2014). Although PTI effectively prevents infection by the majority of potential pathogens, it can be defeated by Gram-negative bacteria, which evolved the type III secretion system (T3SS). The T3SS is a specialized syringe-like apparatus that delivers virulence proteins called the type III secreted effectors (T3SEs) into host cells (Galan *et al.*, 2014). Once inside their hosts, T3SEs directly and indirectly interfere with targets contributing to plant immunity, thereby promoting pathogen entry, colonization and disease development (Feng & Zhou, 2012). The second branch of plant immunity depends on resistance (R) proteins, which were evolved as a counterattack strategy to recognize effector activities (Jacob *et al.*, 2013; Qi & Innes, 2013). Activation of R proteins leads to robust effector-triggered immunity (ETI) that usually involves the development of programmed cell death at the infection sites, called the hypersensitive response (HR). The activation of strong ETI in the presence of R proteins often masks the virulence function of effectors.

The YopJ family of T3SEs has been identified in a large variety of animal and plant pathogens, including *Vibrio*, *Yersinia*, *Aeromonas*, *Salmonella*, *Pseudomonas*, *Ralstonia*, *Xanthomonas* and *Pectobacterium* (Ma *et al.*, 2006). YopJ family effectors share a conserved catalytic triad consisting of histidine, glutamate and cysteine. The catalytic cysteine residue is unexceptionally required for the enzymatic activity and biological function of YopJ family effectors. Although the catalytic triad of YopJ family effectors is identical to that of the C55 family of cysteine proteases (Orth *et al.*, 2000), several family members have been shown to act as an acetyltransferase and modify target proteins in their hosts through acetylation (Mittal *et al.*, 2006; Mukherjee *et al.*, 2006; Trosky *et al.*, 2007; Jones *et al.*, 2008; Lee *et al.*, 2012; Jiang *et al.*, 2013; Lewis *et al.*, 2013; Cheong *et al.*, 2014).

YopJ, the founding member of this effector family in *Yersinia pestis*, acetylates specific lysine, serine and threonine residues of several mitogen-activated protein kinases in animals (Mittal *et al.*, 2006; Mukherjee *et al.*, 2006). Some of the serine and threonine acetylation sites coincide with phosphorylation sites within the activation loop of the corresponding kinases. YopJ therefore suppresses immune signaling by blocking the mitogen-activated kinase phosphorylation relay. In addition to YopJ, AvrA from *Salmonella typhimurium* and VopA from *Vibrio parahemeolyticus* also acetylate target kinases and suppress immune signaling in mammalian cells (Trosky *et al.*, 2007; Jones *et al.*, 2008). YopJ family effectors

produced by plant pathogens are also able to modify their host targets. For example, AvrBsT from *Xanthomonas euvesicatoria* acetylates the microtubule-associated protein ACIP in *Arabidopsis thaliana* and affects its subcellular localization (Cheong *et al.*, 2014).

HopZ1a is a YopJ-like effector produced by the plant pathogen *Pseudomonas syringae*. HopZ1a possesses weak cysteine protease activity using a generic substrate *in vitro* (Ma *et al.*, 2006); however, it also acts as an acetyltransferase and modifies several plant substrates including tubulin (Lee *et al.*, 2012), jasmonate ZIM (JAZ) domain proteins (Jiang *et al.*, 2013), and the pseudokinase ZED1 (Lewis *et al.*, 2013).

YopJ family acetyltransferases use acetyl-coenzyme A (acetyl-CoA) as the acetyl group donor. In general, two mechanisms have been proposed to account for the acetyl-CoA-dependent acetyltransferase activity (Berndsen & Denu, 2005). The first involves the formation of a ternary complex with a lysine on the enzyme attacking the bound acetyl-CoA and subsequently transferring the acetyl group to the substrate. The second mechanism is called the ‘ping-pong’ model, which involves formation of an acetylenzyme intermediate on the catalytic cysteine residue; the acetyl group is then transferred to a substrate. This latter mechanism has been proposed to be used by YopJ (Mukherjee *et al.*, 2006). In support of this hypothesis, autoacetylation was observed in all the YopJ family effectors with demonstrated acetyltransferase activity (Mittal *et al.*, 2010; Tasset *et al.*, 2010; Lee *et al.*, 2012; Cheong *et al.*, 2014). If this model is correct, at least some of the autoacetylation sites would also be required for *trans* acetylation.

The autoacetylation site of a YopJ family effector, PopP2, has been determined by mass spectrometry as lysine383 following the catalytic triad (Tasset *et al.*, 2010). This finding suggests that residues other than the catalytic cysteine can potentially form the acetylenzyme intermediate and subsequently transfer the acetyl group to a substrate. K383 is conserved among most YopJ effectors, including HopZ1a. Substitution of the corresponding residue lysine289 in HopZ1a with an arginine leads to loss of HR triggering and bacterial growth promoting activities in *A. thaliana* (Lee *et al.*, 2012), suggesting that the conserved lysine is also required for the biological function of HopZ1a. However, whether K289 is the autoacetylation site in HopZ1a remains unclear.

In this study, we characterized key residues that contribute to the acetyltransferase activity, co-factor interaction, and biological functions of HopZ1a. Our results showed that K289 is not an autoacetylation site in HopZ1a. Using mass spectrometry, we identified a threonine residue, T346, in the C-terminal region as the main autoacetylation site. In addition, we found that two neighboring serine residues, S349 and S351, play a key role in the enzymatic activity and virulence function of HopZ1a. Importantly, these two serine residues are essential for the interaction of HopZ1a with the co-factor inositol hexakisphosphate (IP6), which has been shown to activate the acetyltransferase activity of several YopJ family effectors in eukaryotic hosts (Mittal *et al.*, 2010; Lee *et al.*, 2012; Cheong *et al.*, 2014). Finally, we demonstrate that S349 and S351 are highly conserved among members of the YopJ family and are also required for the acetyltransferase activity of HopZ3 produced by *P. syringae* pv. *syringae* and PopP2 produced by *Ralstonia solanacerum*. These results suggest

that, in addition to the highly conserved catalytic residues, YopJ family effectors also require conserved serine(s) in the C-terminal domain for their enzymatic activity.

Materials and Methods

Bacterial strains and plasmids

Pseudomonas syringae and *Escherichia coli* strains were grown as described previously (Morgan *et al.*, 2010). Bacterial strains and plasmids used in this study are summarized in Supporting Information Table S1.

Plant material and growth conditions

Arabidopsis thaliana (L.) Heynh seeds were sown in soil and stratified at 4°C for 3 d. The plants were grown in a conditioned growth room (19–21°C, 16-h photoperiod, and relative humidity of 75–80%). Wild-type and mutant *HopZ1a* genes, tagged with 3xFLAG on the N terminus, were cloned into the vector pEG100 (Jiang *et al.*, 2013). The recombinant plasmids were transformed into *Agrobacterium tumefaciens. Arabidopsis thaliana zar1-1* plants were transformed using the floral dip method (Clough & Bent, 1998).

Soybean (*Glycine max* (L.) cv William 82) seeds were surface-sterilized with 10% bleach for 10 min and pre-germinated on wet filter paper at room temperature in the dark for 4 d. Seedlings were transplanted to soil and grown in a conditioned growth room (19–21°C, 16-h photoperiod, and relative humidity of 75–80%).

Protein expression and purification

Wild-type and mutant *HopZ1a* and *PopP2* were cloned into the plasmid vector pRSFDuet-1 (Novagen, Madison, WI, USA) containing a 6× His-SUMO tag, and transformed in *E. coli* strain BL21(DE3). Recombinant 6× His-SUMO-tagged proteins were purified using nickel resin, and the 6× His-SUMO tag was subsequently removed by ULP1 protease as described previously (Jiang *et al.*, 2013).

For nuclear magnetic resonance (NMR) samples, tag-free HopZ1a, HopZ1a(C216A), and HopZ1a(S349AS351A) were further purified by size exclusion chromatography on a Superdex 200 HR 16/60 column (GE Health, Little Chalfont, UK), using buffer containing 20 mM sodium phosphate (pH 7.5) and 150 mM NaCl.

Wild-type and mutant *HopZ3* were cloned in the pET14b vector and expressed in *E. coli* as 6× His-tagged proteins. The 6× His-tagged HopZ3 proteins were purified using a nickel affinity column.

In vitro acetylation assays

An *in vitro* acetylation assay was used to examine the acetyltransferase activity of HopZ1a, PopP2 and HopZ3 to determine the autoacetylation level. One microgram of HopZ1a or PopP2, or 1.5 lμ of HopZ3 was incubated with 1 μl of [14C]-acetyl-CoA (55 μci μmol^{-1}) in 25 μl of reaction buffer (50 mM HEPES (pH 8.0), 10% glycerol, 1 mM DTT, 1 mM PMSF, and 10 mM sodium butyrate) at 30°C for 1 h. The reaction was supplemented with 100 nM

IP6 when appropriate. To determine the *trans* acetylation, 7 μg of MBP-AtJAZ6-HIS was used in each reaction as the substrate. The reactions were stopped by the addition of 2× Laemmli buffer and then subjected to SDS-PAGE. Acetylated proteins were detected by autoradiography as previously described (Jiang *et al.*, 2013). After autoradiography, the protein gels were removed from the filter paper and stained with Coomassie Blue as a loading control.

Nano-UPLC-MS/MS analysis

To identify the autoacetylation site(s) in HopZ1a, 1 μg of tag-free HopZ1a or HopZ1a(C216A) was incubated with C12 acetyl-CoA in a 25-μl reaction system for 1 h. The proteins were precipitated in 100 μl of cold acetone overnight at 20°C. Protein pellets were collected with 30 min of centrifugation at 18 000 ***g***, washed with cold acetone, air-dried, and finally digested with 1 μg of trypsin in 100 μl of ammonium bicarbonate (50 mM; pH 8.0) at 37°C overnight. The trypsin-digested samples were dried to pellets with a speedvac concentrator and then resuspended in 20 μl of 0.1% formic acid solution. A Mud-PIT LC/MS method was employed to analyze these final peptide samples using two-dimension nanoAcquity UPLC (Waters, Milford, MA, USA) and Orbitrap Fusion mass spectrometer (Thermo Fisher, Waltham, MA, USA). The two-dimension nano-UPLC fractionation and separation gradient was described in Drakakaki *et al.* (2012) and the MS survey scan using data-dependent acquisition (DDA) was described previously (Hebert *et al.*, 2014). To confirm the specific acetylation site, the same samples were re-analyzed using a targeted scan method, with which the MS2 spectra were acquired using Orbitrap, instead of an ion trap, with a resolution set at 30 000.

All raw MS data were processed with PROTEOME DISCOVERER version 1.4 (Thermo Fisher) to generate mgf files that were used in a Mascot search against the HopZ1a protein sequence (Matrix Science Inc., Boston, MA, USA). Mascot search parameters allowed various modifications including N-terminal acetylation, oxidation (M), Gln→pyro-Glu (N-term Q), Glu→pyro-Glu (N-term E), K-acetylation, S-acetylation, T-acetylation and H-acetylation. HopZ1a(C216A) was used as a control to identify the HopZ1a-specific acetylation site(s).

Pseudomonas syringae infection assays

The leaves of 5-wk-old *A. thaliana* plants were infiltrated with bacterial suspensions at OD_{600} = 0.0001 (*c*. 1×10^5 CFU ml^{-1}) for *Pseudomonas syringae* pv. *tomato* strain DC3000 (*Pto*DC3000) and OD_{600} = 0.005 for *Pseudomonas syringae* pv. *syringae* strain B728aΔZ3 (*Psy*B728aΔZ3) (*c*. 5×10^6 CFU ml^{-1}). The inoculated plants were transferred to a growth chamber (22°C, 16 h: 8 h, light : dark regime, and 90% humidity), and the bacterial populations were determined as colony forming units (cfu) per cm^2 3 d after inoculation using a previously described procedure (Morgan *et al.*, 2010).

To test the HR-triggering activity of HopZ1a mutants, leaves of 5-wk-old *A. thaliana* plants (ecotype Columbia (Col-0)) and fully expanded primary leaves of 14-d-old soybean (cultivar Williams 82) were infiltrated with bacterial suspensions at an OD_{600} = 0.2 (*c*. 2×10^8 CFU ml^{-1}) for *Pto*D28E (Cunnac *et al.*, 2011) and OD_{600} = 0.1 (*c*. 1×10^8 CFU ml^{-1}) for

*Pgy*BR1-O1. Cell death symptoms within the infiltrated areas were monitored at 24–48 h after inoculation.

Callose deposition analysis

Leaves of 5-wk-old transgenic *A. thaliana zar1-1* plants expressing wild-type or mutant HopZ1a were infiltrated with water or 1 μM flg22 (PhytoTechnology Laboratories, Shawnee Mission, KS, USA). Sixteen hours after the treatment, the infiltrated leaves were fixed in an ethanol : acetic acid solution as previous described (Millet *et al.*, 2010), and stained with 0.01% aniline blue (Sigma-Aldrich). Callose deposition in the leaves was observed under UV using a BX51 fluorescent microscope (Olympus, Center Valley, PA, USA). In each treatment, 12 independent images were analyzed and the numbers of callose deposits were determined using IMAGEJ.

Stomatal aperture analysis

Stomatal apertures were analyzed using a modified protocol based on a procedure described by Liu *et al.* (2009). Leaf discs of 4-wk-old transgenic *A. thaliana zar1-1* plants expressing wild-type or mutant HopZ1a were incubated, with the abaxial side facing down, in an MES buffer (10 mM KCl, 0.2 mM $CaCl_2$, 10 mM MES-KOH (pH 6.5) and 0.025% silvet-77). Full opening of the stomata was induced by placing the discs under illumination for at least 2 h before the buffer was replaced with fresh MES buffer containing 10 μM flg22. Leaf discs were then incubated with flg22 under illumination for another 2 h. Medical adhesive (Hollister, Libertyville, IL, USA) was applied to a slide and the leaf discs were placed on the adhesive with the abaxial side facing down. A razor blade was then used to carefully scrape away the upper epidermis and the stomata were immediately observed using a Primo Star microscope (Zeiss, Oberkochen, Germany). At least ten independent images were taken for each treatment and at least six stomata per image were analyzed for aperture, which was expressed as the ratio of width over length.

1D proton (^{1}H) NMR

For NMR experiments, 0.1 mM purified wild-type and mutant HopZ1a proteins, in the absence or presence of 1 mM IP6, were dissolved in 500 μl of buffer containing 20 mM sodium phosphate (pH 7.5), 150 mM NaCl and 10% D_2O. 1D proton NMR spectra (256 scans each) were collected for HopZ1a proteins on a Bruker Advance 600 MHz NMR spectrometer (Bruker Inc., Billerica, MA, USA) equipped with a TXI probe at 25°C. The NMR spectra were then processed and analyzed using the TOPSIN software (Bruker).

Results

Characterization of potential autoacetylation sites in HopZ1a

Previously, a conserved lysine residue, K383, in PopP2 was identified as the autoacetylation site (Tasset *et al.*, 2010). The corresponding K289 in HopZ1a was also suggested to be the autoacetylation site, as autoacetylation was not observed from GST-HopZ1a(K289R) *in vitro* (Lee *et al.*, 2012). To confirm the role of K289, we purified tag-free HopZ1a(K289R) proteins and examined the autoacetylation activity using an *in vitro* acetylation assay in the presence of C14-labeled acetyl-CoA and the eukaryotic co-factor IP6. Inconsistent with the

previous report, we did not observe reduced autoacetylataion from HopZ1a(K289R) (Fig. 1a). Instead, a significantly stronger autoacetylation signal was consistently observed from this mutant. This result suggests that: (1) K289 is not required for autoacetylation of HopZ1a; (2) K289 is unlikely to be an autoacetylation site, at least not a major one, of HopZ1a.

To identify the autoacetylation site(s), we analyzed HopZ1a and the catalytic mutant HopZ1a(C216A) using mass spectrometry. This experiment revealed many potential acetylation sites, most of which were lysine, threonine and serine residues, in both wild type and the catalytic mutant (Table S2). These residues are probably being acetylated independent of the enzymatic activity of HopZ1a, and therefore were not considered as candidate autoacetylation sites. The only exception is the peptide of 335–356 aa, which showed a mass shift of 42 atomic mass units (amu), possibly as a result of acetylation, only in wild-type HopZ1a. This peptide therefore probably contains a residue that is acetylated in a HopZ1a acetyltransferase-dependent manner. Fragmentation analysis further identified threonine346 (T346) as the acetylation site (Fig. 1b).

Our mass spectrometry analysis allowed us to detect a potential acetylation in the peptide 289–301 aa, which contains K289 (Table S2). However, further fragmentation analysis suggested that T295, instead of K289, was the acetylated site. Moreover, this acetylated peptide was identified in both wild-type HopZ1a and the catalytic mutant HopZ1a(C216A), suggesting that this acetylation is not dependent on the enzymatic activity of HopZ1a. These results confirmed that K289 is not an autoacetylation site of HopZ1a.

To further confirm the role of T346, we constructed the mutant HopZ1a(T346A) and examined its autoacetylation *in vitro*. To our surprise, HopZ1a(T346A) exhibited a similar level of autoacetylation to wild-type HopZ1a (Fig. 1c). YopJ family effectors have been shown to be able to acetylate several amino acids including serine, threonine and lysine (Mukherjee *et al.*, 2006; Trosky *et al.*, 2007; Jones *et al.*, 2008; Tasset *et al.*, 2010). In close proximity to T346, the acetylated tryptic peptide contains additional residues, that is, S344, S349 and S351, that could potentially be acetylated, especially when T346 is mutated. We therefore systematically mutated these residues and examined the mutants using an *in vitro* acetylation assay. The autoacetylation signal exhibited an *c*. 70% reduction in HopZ1a (S349AS351A) compared with wild-type HopZ1a, but was not reduced relative to wild type in HopZ1a(S344A), HopZ1a (S349A) or HopZ1a(S351A) (Fig. 1c).

Because the mutant HopZ1a(S349AS351A) exhibited a significantly reduced level of autoacetylation, we next examined its *trans* acetylation using AtJAZ6 as the substrate (Jiang *et al.*, 2013). Our experiments showed an almost complete loss of At-JAZ6 acetylation by HopZ1a(S349AS351A) (Fig. 2). Similar to the data shown in Fig. 1a, the mutant HopZ1a(K289R) exhibited an enhanced level of autoacetylation; however, *trans* acetylation of AtJAZ6 by HopZ1a(K289R) was significantly weakened (*c*. 50% reduction) (Fig. 2), suggesting that K289R specifically contributes to *trans* acetylation.

Because K289 and S349/S351 both contribute to the acetyltransferase activity of HopZ1a, but in different ways, we examined a triple mutant HopZ1a(K289RS349AS351A) and found

that this mutant had completely lost both auto- and *trans* acetylation, similar to the catalytic mutant HopZ1a(C216A) (Fig. 2). These results suggest that S349A and S351 are important for the enzymatic activity of HopZ1a in general, whereas K289 specifically contributes to *trans* acetylation, possibly in a later step of the enzymatic reaction.

S349 and S351 are required for HR-triggering activity of HopZ1a in plants

In *A. thaliana* Col-0, HopZ1a-elicited HR depends on the R protein HopZ-activated resistance 1 (ZAR1) (Lewis *et al.*, 2010). Furthermore, this HR-triggering activity is abrogated in the catalytic mutant HopZ1a(C216A) (Ma *et al.*, 2006). Based on the results from the acetylation assays, we hypothesized that S349 and S351 would also be required for HopZ1a to trigger the HR in plants. To test this hypothesis, we introduced wild-type or mutant *HopZ1a* genes into *Pto*D28E, a mutant of wild-type strain DC3000 with 28 type III effectors deleted (Cunnac *et al.*, 2011). *Pto*D28E still has a functional type III secretion apparatus, allowing the delivery of HopZ1a or its mutants into plant cells; however, the absence of the endogenous type III effectors minimizes their potential interference on the HR-triggering phenotype by HopZ1a. Bacterial infiltration assays showed that *Pto*D28E expressing the mutant HopZ1a (S349AS351A) was no longer able to induce cell death in *A. thaliana* Col-0 (Fig. 3a). A similar phenotype was also observed in soybean (*Glycine max*) (Fig. S1), suggesting that S349 and S351 are required for HopZ1a to elicit the HR in plant hosts. Consistent with the *in vitro* acetylation data, the triple mutant HopZ1a(K289RS349AS351A) also lost the HR-triggering activity (Fig. 3a). In contrast, mutants including HopZ1a(T346A), Z1a(S349A) and Z1a(S351A), which exhibited unaltered acetylation activity, were still able to trigger the HR (Fig. S2).

To provide a quantitative measurement of the contribution of S349 and S351 to the HopZ1a-triggered defense response, we determined the bacterial population of *Pto*DC3000 expressing wild-type or mutant forms of HopZ1a in *A. thaliana* Col-0. Consistent with the loss of the cell death phenotype, *Pto*DC3000 (HopZ1a(S349AS351A)) and *Pto*DC3000(HopZ1a(K289RS34 9AS351A)) multiplied to a similar level as *Pto*DC3000 carrying the empty vector (EV) or expressing the catalytic mutant HopZ1a(C216A) (Fig. 3b). Interestingly, although HopZ1a (K289R) was unable to elicit cell death in the infiltrated leaves (Fig. 3a), the population of *Pto*DC3000(HopZ1a (K289R)) was *c*. 5–10-fold smaller than that of *Pto*DC3000 (HopZ1a(S349AS351A)) or *Pto*DC3000(HopZ1a(C216A)) (Fig. 3b). These data suggest that HopZ1a(K289R) could still elicit a weak defense response, which is consistent with the partial loss of *trans* acetylation in HopZ1a(K289R) (Fig. 2). The observed changes in defense-eliciting activity of HopZ1a mutants were not attributable to the altered expression levels of the mutant proteins, as the expression of mutant proteins was confirmed by western blots (Fig. S3).

S349 and S351 are required for the virulence activities of HopZ1a

In the absence of the R gene *zar1*, HopZ1a promotes *P. syringae* infection in *A. thaliana* (Jiang *et al.*, 2013) and inhibits plant cell wall callose deposition induced by flg22, the major PAMP of *P. syringae* (Lee *et al.*, 2012). We next examined the contribution of S349 and S351 to the virulence activities of HopZ1a.

Arabidopsis thaliana transgenic plants expressing wild-type or mutant HopZ1a were generated in the *zar1-1* background (Fig. S4). These plants were infiltrated with flg22 and the numbers of callose deposits were numerated. Our results showed that HopZ1a(S349AS351A) lost the ability to suppress callose deposition triggered by flg22, similar to the catalytic mutant HopZ1a (C216A) (Fig. 4a). The mutant HopZ1a(K289R) also lost the ability to suppress callose deposition (Fig. 4a), suggesting that *trans* acetylation is responsible for the PTI suppression activity of HopZ1a.

To further confirm that S349 and S351 are required for HopZ1a to promote bacterial infection, we introduced wild-type and mutants of HopZ1a into *Psy*B728aΔZ3 (Vinatzer *et al.*, 2006) and evaluated the bacterial populations in *A. thaliana zar1-1* plants. *Psy*B728aΔZ3 is a nonpathogen of *A. thaliana* Col-0 and thus serves as a useful tool to evaluate the virulence activity of HopZ1a. Expression of HopZ1a promoted bacterial infection and the population of *Psy*B728aΔZ3(HopZ1a) was 5-fold greater than that of *Psy*B728aΔZ3 (Fig. 4b). This growth promotion activity was lost in the mutants HopZ1a (S349AS351A), HopZ1a(K289R) and HopZ1a(K289RS349 AS351A) (Fig. 4b).

S349 and S351 are required for the suppression of stomatal closure by HopZ1a

Bacterial infection induces closure of plant stomata, which could prevent bacterial entry. In *P. syringae*, T3SEs HopM1 (Lozano-Duran *et al.*, 2014) and HopF2 (Hurley *et al.*, 2014), as well as the phytotoxin coronatine (COR) (Melotto *et al.*, 2006), can promote infection by interfering with stomatal defense. In particular, COR induces the degradation of JAZ proteins and activates jasmonate (JA) signaling, thus leading to reopening of stomata to facilitate bacterial entry (Melotto *et al.*, 2006; Zheng *et al.*, 2012). HopZ1a is also able to activate JA signaling by targeting the JAZ proteins (Jiang *et al.*, 2013); however, whether HopZ1a could manipulate stomatal opening is unknown.

To examine whether HopZ1a is able to suppress stomatal defense, we measured the stomatal aperture in leaves of transgenic *A. thaliana zar1-1* expressing wild-type or mutant HopZ1a after infiltration with flg22, which induces stomatal closure (Melotto *et al.*, 2006). Two hours after flg22 treatment, the width : length ratio of each stoma ($n = 60$) in the leaves was determined. Consistent with the JA-activating ability of HopZ1a, expression of HopZ1a led to a wider stomatal aperture in the leaves (Fig. 5a,b). In contrast, the mutants HopZ1a(S349AS351A), HopZ1a (K289R) and the catalytic mutant HopZ1a(C216A) were unable to increase stomatal aperture (Fig. 5a,b). Further experiments confirmed that stomata were closed upon flg22 treatment in transgenic *A. thaliana* expressing HopZ1a(C216A) in a similar manner as in *A. thaliana zar1-1* plants (Fig. S5). These results demonstrate that HopZ1a can suppress stomatal defense in an enzymatic activity-dependent manner. Importantly, S349 and S351 are required for this virulence activity, probably as a consequence of their essential role in the acetyltransferase activity of HopZ1a.

Residues S349 and S351 are required for the interaction with the co-factor IP6

Even though our mass spectrometry data did not reveal S349 and S351 acetylation *in vitro*, these residues are required for the enzymatic activity of HopZ1a. One possibility is that S349 and S351 may affect the protein conformation of HopZ1a. To test this hypothesis, we

compared the conformations of HopZ1a and HopZ1a(S349AS351A) in solution using 1D proton NMR, which is a powerful analytical tool widely used to characterize the structural and dynamic behaviors of proteins in solution state. The ^{1}H chemical shifts are highly sensitive to local changes in the chemical environment, therefore offering an important parameter to evaluate protein conformational states and protein–ligand interactions. In general, NMR signals in the aromatic region serve as a good indicator of the folding status of a protein (Pruitt *et al.*, 2009).

The NMR spectra of purified HopZ1a, HopZ1a(C216A) and HopZ1a(S349AS351A) proteins did not exhibit significant differences (Figs 6a, S6), suggesting that the substitutions of S349 and S351 did not affect the overall conformation of HopZ1a. However, we observed extensive changes in NMR spectra of HopZ1a in the presence of the co-factor IP6. The addition of IP6 to HopZ1a resulted in a much wider dispersion of NMR signals (Fig. S7) and peak shifts in the aromatic region (Fig. 6). These chemical shift changes, together with the emergence of both high-frequency and low-frequency NMR signals, indicate that IP6 binds to HopZ1a to induce a more compact folding state of HopZ1a. Interestingly, such an IP6-induced conformational change is independent of the catalytic residue, as the same spectral changes were also observed for the catalytic mutant HopZ1a(C216A) in the presence of IP6 (Fig. 6a). By contrast, the NMR spectrum of HopZ1a(S349AS351A) was not altered by IP6 (Fig. 6a), suggesting that S349 and S351 are required for the conformational changes of HopZ1a induced by IP6, presumably from an inactivated state to a more compact, activated state.

To further confirm that S349 and S351 are essential for IP6-mediated activation of HopZ1a enzymatic activity, we conducted *in vitro* acetylation assays and compared the autoacetylation levels of HopZ1a (S349AS351A) in the presence and absence of IP6. Interestingly, although the autoacetylation level of wild-type HopZ1a was enhanced *c*. 40% in the presence of IP6, such an enhancement was not observed for HopZ1a(S349AS351A) (Fig. 6b). These data support a model in which S349 and S351 affect HopZ1a enzymatic activity at least partially through an interaction with IP6.

Conserved serine residues in other YopJ family effectors are required for their acetyltransferase activity

Sequence alignment revealed that S349 and S351 are conserved in most YopJ family effectors (Figs 7a, S8). Therefore, they may also be important for the enzymatic activity of other YopJ family members. To test this hypothesis, we introduced mutations on the corresponding serine residue(s) in two YopJ family effectors, PopP2 of *Ralstonia solanacerum* and HopZ3 of *P. syringae* pv. *syringae*, and examined them for their autoacetylation *in vitro*. PopP2 contains both serines at sites 447 and 449 and the mutant PopP2(S447AS449A) is no longer autoacetylated (Fig. 7b). HopZ3 is a YopJ family effector that is also produced by *P. syringae* pv. *syringae* and is evolutionarily related to HopZ1a (Ma *et al.*, 2006). We show here that HopZ3 possesses an acetyltransferase activity *in vitro* (Fig. 7c). HopZ3 has one of the conserved serines at site 386 which corresponds to S351 of HopZ1a. The mutant HopZ3(S386A) also lost autoacetylation ability (Fig. 7c). These data

suggest that serine residues play a conserved role in YopJ family effectors and are required for their acetyltransferase activities.

Discussion

Several YopJ family effectors have been shown to be acetyltransferases, including HopZ1a. Based on the proposed 'ping-pong' model, autoacetylation of YopJ family effectors could generate an acetylenzyme intermediate (Mukherjee *et al.*, 2006) for the subsequent transfer of the acetyl group to substrates. K289 was previously hypothesized to be the autoacetylation site of HopZ1a (Lee *et al.*, 2012). However, K289 was not identified as being acetylated in our mass spectrometry analysis. Importantly, *in vitro* assays showed that autoacetylation of HopZ1a was not weakened by the K289R mutation. This is inconsistent with the complete loss of autoacetylation observed in HopZ1a(K289R) in a previous study (Lee *et al.*, 2012). This discrepancy could be explained by the different constructs used in this study (i.e. tag-free proteins) and the previous publication (GST-tagged proteins). Nonetheless, we observed a significant decrease in *trans* acetylation of AtJAZ6 by HopZ1a(K289R), suggesting that K289 still plays an important role in the biological function of HopZ1a, but probably not by serving as the autoacetylation site. A similar observation was also made in another YopJ family effector, AvrBsT, where the corresponding lysine residue K282 is required for *trans* acetylation, but not for autoacetylation (Cheong *et al.*, 2014). Interestingly, we constantly observed enhanced autoacetylation signals from HopZ1a (K289R) compared with wild-type HopZ1a. It is possible that other residues that are normally not acetylated in HopZ1a could be acetylated upon the mutation of K289, or that the autoacetylation site is locked in the acetylenzyme intermediate form because of suppression of *trans* acetylation caused by the K289R substitution.

Using mass spectrometry, we identified T346 as the only autoacetylation site of HopZ1a. This experiment was repeated twice in two mass spectrometry facilities with identical results. However, autoacetylation of HopZ1a was not weakened upon mutation of T346. This result suggests that another residue(s) could serve as a supplementary acetylation site(s) when T346 is absent. Indeed, T346 is not conserved in YopJ family effectors (Fig. 7a and S8). Nonetheless, mutations in two neighboring residues, S349 and S351, significantly affect the enzymatic activity of HopZ1a. These two serine residues may supplement T346 as the alternative autoacetylation site(s) in the mutant HopZ1a (T346A). This possibility is supported by the observation that substitution of the corresponding serine residues in another two YopJ family effectors, PopP2 and HopZ3, abolished their autoacetylation. Another interesting observation is that the triple mutant HopZ1a(K289RS349AS351A) is completely abolished for autoacetylation. It seems likely that K289 indirectly regulates, but does not determine, the enzymatic activity of HopZ1a together with the serine residues.

The acetyltransferase activity of several YopJ family effectors can be activated by IP6 as a co-factor (Mittal *et al.*, 2010; Lee *et al.*, 2012; Cheong *et al.*, 2014). As a natural product that is present in relatively high abundance in eukaryotes, the absence of IP6 in bacteria suggests that the enzymatic activity of YopJ family effectors is activated after they are delivered into the hosts (Mittal *et al.*, 2010). IP6 induces conformational changes of AvrA

(Mittal *et al.*, 2010). Using NMR, we also observed the transition of HopZ1a to a more folded state in the presence of IP6. Importantly, our data demonstrated that S349 and S351 are required for HopZ1a association with IP6 and/or IP6-induced conformation changes. Consistent with a role in IP6-induced conformational changes, the enhancement of HopZ1a activity by IP6 was lost in HopZ1a(S349AS351A). Furthermore, the association of HopZ1a with IP6 is not dependent on the catalytic residue C216, suggesting that the function of these C-terminal residues is distinctive from that of the catalytic residues.

Small-molecule-induced allosteric regulation is a common mechanism to regulate enzymatic activities. IP6 has been implicated as an important component in the regulation of different proteins. For instance, IP6 induces a conformational change of the normally disordered RNA editing enzyme hADAR2 (Macbeth *et al.*, 2005), a vesicle membrane protein, synaptotagmin I (Joung *et al.*, 2012), and a sensory perception-related protein, arrestin (Zhuang *et al.*, 2010). IP6 is also known to activate bacterial toxins, including repeats in toxin (RTX) produced by *Vibrio cholera* (Lupardus *et al.*, 2008) and toxin A produced by *Clostridium difficile (*Pruitt *et al.*, 2009) after they enter animal cells. The known IP6-binding motifs often include a basic pocket with polar residues, such as serine, which are involved in stabilizing the protein–IP6 interaction. Therefore, it is likely that the highly conserved serine residues identified in this study are part of the IP6-binding pocket in YopJ family effectors, and the resultant conformation changes enhance their enzymatic activities.

The conservation of serine residues among YopJ effectors and the requirement for them for the enzymatic activities of PopP2 and HopZ3 suggest that the serine residues serve an essential role in the activity of this family of acetyltransferases. The presence of a conserved C-terminal domain has been proposed previously (Mukherjee *et al.*, 2007). Our analyses suggest that the conserved serine residues in the C-terminal domain may contribute to the activation of acetyltransferase activity after the YopJ family effectors enter eukaryotic hosts via co-factor interaction. As the autoacetylation activities are almost completely lost in PopP2(S447AS449A) and HopZ3(386A), it is possible that the analogous serines in PopP2 and HopZ3 also serve as autoacetylation sites.

In summary, we report two conserved serine residues in the C-terminal domain of HopZ1a that are required for the biological function of HopZ1a, as demonstrated by the loss of HR-triggering ability, and suppression of defense responses including callose deposition and stomatal closure. We showed that these serine residues are important for the enzymatic activity of HopZ1a and are indispensable for IP6-induced activation in eukaryotic hosts. This work provides insights into enzymatic activity regulation of an important family of bacterial effectors in the hosts. As bacterial effectors are potent virulence factors during infection, this knowledge may potentially be applied to the screening of chemical inhibitors of YopJ family effectors.

Supplementary Material

Refer to Web version on PubMed Central for supplementary material.

Acknowledgments

This work was supported by funds from the University of California-Riverside and NSF grant IOS-0847870 to W.M, NSF grant MCB-1054298 and NIH grant RO1GM092772 to G.C., and Basil O'Connor Starting Scholar Research Award, March of Dimes Foundation, and University of California-Riverside start-up funds to J.S. The PopP2 and PopP2(C321A) constructs were kindly provided by Dr Jonathan Jones. The *P. syringae* strains *Pto*D28E and B728aDZ3 were kindly provided by Drs Alan Collmer and Jean Greenberg. We thank Dr Dan Borchardt for technical assistance with the NMR analysis.

References

Berndsen CE, Denu JM. Assays for mechanistic investigations of protein/histone acetyltransferases. Methods. 2005; 36:321–331. [PubMed: 16085424]

Bohm H, Albert I, Fan L, Reinhard A, Nurnberger T. Immune receptor complexes at the plant cell surface. Current Opinion in Plant Biology. 2014; 20:47–54. [PubMed: 24835204]

Cheong MS, Kirik A, Kim J-G, Frame K, Kirik V, Mudgett MB. AvrBsT acetylates Arabidopsis ACIP1, a protein that associates with microtubules and is required for immunity. PLoS Pathogens. 2014; 10:e1003952. [PubMed: 24586161]

Clough SJ, Bent AF. Floral dip: a simplified method for Agrobacterium-mediated transformation of *Arabidopsis thaliana*. Plant Journal. 1998; 16:735–743. [PubMed: 10069079]

Cunnac S, Chakravarthy S, Kvitko BH, Russell AB, Martin GB, Collmer A. Genetic disassembly and combinatorial reassembly identify a minimal functional repertoire of type III effectors in *Pseudomonas syringae*. Proceedings of the National Academy of Sciences, USA. 2011; 108:2975–2980.

Drakakaki G, van de Ven W, Pan S, Miao Y, Wang J, Keinath NF, Weatherly B, Jiang L, Schumacher K, Hicks G, et al. Isolation and proteomic analysis of the SYP61 compartment reveal its role in exocytic trafficking in Arabidopsis. Cell Research. 2012; 22:413–424. [PubMed: 21826108]

Feng F, Zhou JM. Plant-bacterial pathogen interactions mediated by type III effectors. Current Opinion in Plant Biology. 2012; 15:469–476. [PubMed: 22465133]

Galan JE, Lara-Tejero M, Marlovits TC, Wagner S. Bacterial type III secretion systems: specialized nanomachines for protein delivery into target cells. Annual Review of Microbiology. 2014; 68:415–438.

Hebert AS, Richards AL, Bailey DJ, Ulbrich A, Coughlin EE, Westphall MS, Coon JJ. The one hour yeast proteome. Molecular & Cellular Proteomics: MCP. 2014; 13:339–347. [PubMed: 24143002]

Hurley B, Lee D, Mott A, Wilton M, Liu J, Liu YC, Angers S, Coaker G, Guttman DS, Desveaux D. The *Pseudomonas syringae* type III effector HopF2 suppresses Arabidopsis stomatal immunity. PLoS One. 2014; 9:e114921. [PubMed: 25503437]

Jacob F, Vernaldi S, Maekawa T. Evolution and conservation of plant NLR functions. Frontiers in Immunology. 2013; 4:297. [PubMed: 24093022]

Jiang S, Yao J, Ma K-W, Zhou H, Song J, He SY, Ma W. Bacterial effector activates jasmonate signaling by directly targeting JAZ transcriptional repressors. PLoS Pathogens. 2013; 9:e1003715. [PubMed: 24204266]

Jones JDG, Dangl JL. The plant immune system. Nature. 2006; 444:323–329. [PubMed: 17108957]

Jones RM, Wu H, Wentworth C, Luo L, Collier-Hyams L, Neish AS. Salmonella AvrA coordinates suppression of host immune and apoptotic defenses via JNK pathway blockade. Cell Host & Microbe. 2008; 3:233–244. [PubMed: 18407067]

Joung M-J, Mohan SK, Yu C. Molecular level interaction of inositol hexaphosphate with the C2B domain of human synaptotagmin I. Biochemistry. 2012; 51:3675–3683. [PubMed: 22475172]

Lee AH-Y, Hurley B, Felsensteiner C, Yea C, Ckurshumova W, Bartetzko V, Wang PW, Quach V, Lewis JD, Liu YC, et al. A bacterial acetyltransferase destroys plant microtubule networks and blocks secretion. PLoS Pathogens. 2012; 8:e1002523. [PubMed: 22319451]

Lewis JD, Lee AH-Y, Hassan JA, Wan J, Hurley B, Jhingree JR, Wang PW, Lo T, Youn J-Y, Guttman DS, et al. The Arabidopsis ZED1 pseudokinase is required for ZAR1-mediated immunity induced by the *Pseudomonas syringae* type III effector HopZ1a. Proceedings of the National Academy of Sciences, USA. 2013; 110:18722–18727.

Lewis JD, Wu R, Guttman DS, Desveaux D. Allele-specific virulence attenuation of the *Pseudomonas syringae* HopZ1a type III effector via the Arabidopsis ZAR1 resistance protein. PLoS Genetics. 2010; 6:e1000894. [PubMed: 20368970]

Liu J, Elmore JM, Fuglsang AT, Palmgren MG, Staskawicz BJ, Coaker G. RIN4 functions with plasma membrane H^+-ATPases to regulate stomatal apertures during pathogen attack. PLoS Biology. 2009; 7:e1000139. [PubMed: 19564897]

Lozano-Duran R, Bourdais G, He SY, Robatzek S. The bacterial effector HopM1 suppresses PAMP-triggered oxidative burst and stomatal immunity. New Phytologist. 2014; 202:259–269. [PubMed: 24372399]

Lupardus PJ, Shen A, Bogyo M, Garcia KC. Small molecule-induced allosteric activation of the *Vibrio cholerae* RTX cysteine protease domain. Science. 2008; 322:265–268. [PubMed: 18845756]

Ma W, Dong FFT, Stavrinides J, Guttman DS. Type III effector diversification via both pathoadaptation and horizontal transfer in response to a coevolutionary arms race. PLoS Genetics. 2006; 2:e0020209.

Macbeth MR, Schubert HL, VanDemark AP, Lingam AT, Hill CP, Bass BL. Inositol hexakisphosphate is bound in the ADAR2 core and required for RNA editing. Science. 2005; 309:1534–1539. [PubMed: 16141067]

Melotto M, Underwood W, Koczan J, Nomura K, He SY. Plant stomata function in innate immunity against bacterial invasion. Cell. 2006; 126:969–980. [PubMed: 16959575]

Millet YA, Danna CH, Clay NK, Songnuan W, Simon MD, Werck-Reichhart D, Ausubel FM. Innate immune responses activated in Arabidopsis roots by microbe-associated molecular patterns. Plant Cell. 2010; 22:973–990. [PubMed: 20348432]

Mittal R, Peak-Chew S-Y, McMahon HT. Acetylation of MEK2 and IjB kinase (IKK) activation loop residues by YopJ inhibits signaling. Proceedings of the National Academy of Sciences, USA. 2006; 103:18574–18579.

Mittal R, Peak-Chew SY, Sade RS, Vallis Y, McMahon HT. The acetyltransferase activity of the bacterial toxin YopJ of *Yersinia* is activated by eukaryotic host cell inositol hexakisphosphate. Journal of Biological Chemistry. 2010; 285:19927–19934. [PubMed: 20430892]

Morgan RL, Zhou H, Lehto E, Nguyen N, Bains A, Wang X, Ma W. Catalytic domain of the diversified *Pseudomonas syringae* type III effector HopZ1 determines the allelic specificity in plant hosts. Molecular Microbiology. 2010; 76:437–455. [PubMed: 20233307]

Mukherjee S, Hao Y-H, Orth K. A newly discovered post-translational modification – the acetylation of serine and threonine residues. Trends in Biochemical Sciences. 2007; 32:210–216. [PubMed: 17412595]

Mukherjee S, Keitany G, Li Y, Wang Y, Ball HL, Goldsmith EJ, Orth K. *Yersinia* YopJ acetylates and inhibits kinase activation by blocking phosphorylation. Science. 2006; 312:1211–1214. [PubMed: 16728640]

Orth K, Xu Z, Mudgett MB, Bao ZQ, Palmer LE, Bliska JB, Mangel WF, Staskawicz B, Dixon JE. Disruption of signaling by *Yersinia* effector YopJ, a ubiquitin-like protein protease. Science. 2000; 290:1594–1597. [PubMed: 11090361]

Pruitt RN, Chagot B, Cover M, Chazin WJ, Spiller B, Lacy DB. Structure–function analysis of inositol hexakisphosphate-induced autoprocessing in *Clostridium difficile* toxin A. Journal of Biological Chemistry. 2009; 284:21934–21940. [PubMed: 19553670]

Qi D, Innes RW. Recent advances in plant NLR structure, function, localization, and signaling. Frontiers in Immunology. 2013; 4:348. [PubMed: 24155748]

Spoel SH, Dong X. How do plants achieve immunity? Defence without specialized immune cells. Nature Reviews Immunology. 2012; 12:89–100.

Tasset C, Bernoux M, Jauneau A, Pouzet C, Brière C, Kieffer-Jacquinod S, Rivas S, Marco Y, Deslandes L. Autoacetylation of the *Ralstonia solanacearum* effector PopP2 targets a lysine residue essential for RRS1-R-mediated immunity in Arabidopsis. PLoS Pathogens. 2010; 6:e1001202. [PubMed: 21124938]

Trosky JE, Li Y, Mukherjee S, Keitany G, Ball H, Orth K. VopA Inhibits ATP binding by acetylating the catalytic loop of MAPK kinases. Journal of Biological Chemistry. 2007; 282:34299–34305. [PubMed: 17881352]

Vinatzer BA, Teitzel GM, Lee M-W, Jelenska J, Hotton S, Fairfax K, Jenrette J, Greenberg JT. The type III effector repertoire of *Pseudomonas syringae* pv. *syringae* B728a and its role in survival and disease on host and non-host plants. Molecular Microbiology. 2006; 62:26–44. [PubMed: 16942603]

Zheng, X-y; Spivey Natalie, W.; Zeng, W.; Liu, P-P.; Fu Zheng, Q.; Klessig Daniel, F.; He Sheng, Y.; Dong, X. Coronatine promotes *Pseudomonas syringae* virulence in plants by activating a signaling cascade that inhibits salicylic acid accumulation. Cell Host & Microbe. 2012; 11:587–596. [PubMed: 22704619]

Zhuang T, Vishnivetskiy SA, Gurevich VV, Sanders CR. Elucidation of inositol hexaphosphate and heparin interaction sites and conformational changes in Arrestin-1 by solution nuclear magnetic resonance. Biochemistry. 2010; 49:10473–10485. [PubMed: 21050017]

Zipfel C. Plant pattern-recognition receptors. Trends in Immunology. 2014; 35:345–351. [PubMed: 24946686]

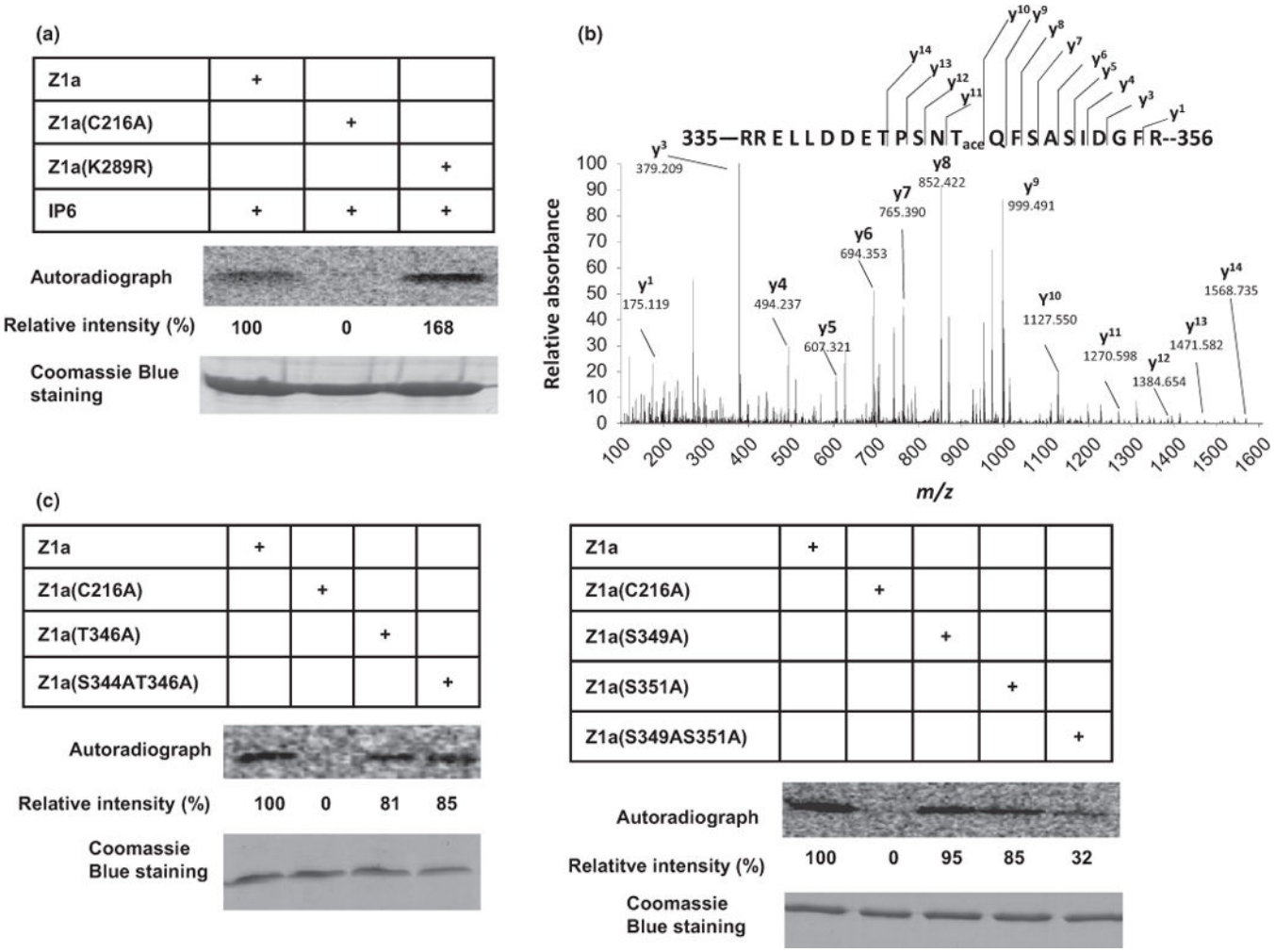

Fig. 1.

Identification of the autoacetylation site(s) in HopZ1a. (a) K289 is not required for the autoacetylation of HopZ1a. Tag-free HopZ1a, the catalytic mutant HopZ1a(C216A), and HopZ1a(K289R) were purified from *Escherichia coli* and subjected to *in vitro* acetylation assays using C14-acetyl CoA. The reaction was supplemented with inositol hexakisphosphate (IP6) as a co-factor. The acetylated proteins were detected by autoradiography after exposure at −80°C for 5 d. Numbers underneath the autoradiograph indicate relative acetylation levels of HopZ1a mutants compared with wild-type protein (100%). Equal loading of the proteins was confirmed by Coomassie Blue staining. (b) T346 is the prominent acetylation site in HopZ1a. Tag-free HopZ1a and HopZ1a(C216A) were incubated with IP6 and acetyl CoA before being subjected to MS/MS spectrometric analysis. The y ions are marked in the spectrum and illustrated along the peptide sequence (parent ion: *m/z* 847.4025, 3+). T346 acetylation was not detected in the catalytic mutant HopZ1a (C216A). (c) Substitutions of S349 and S351 greatly reduced the autoacetylation level of HopZ1a. T346 and its neighboring serine residues S344, S349 and S351 were systematically mutated and tested for autoacetylation activity using the *in vitro* acetylation assay with the

reactions supplemented with IP6. These experiments were repeated three times with similar results.

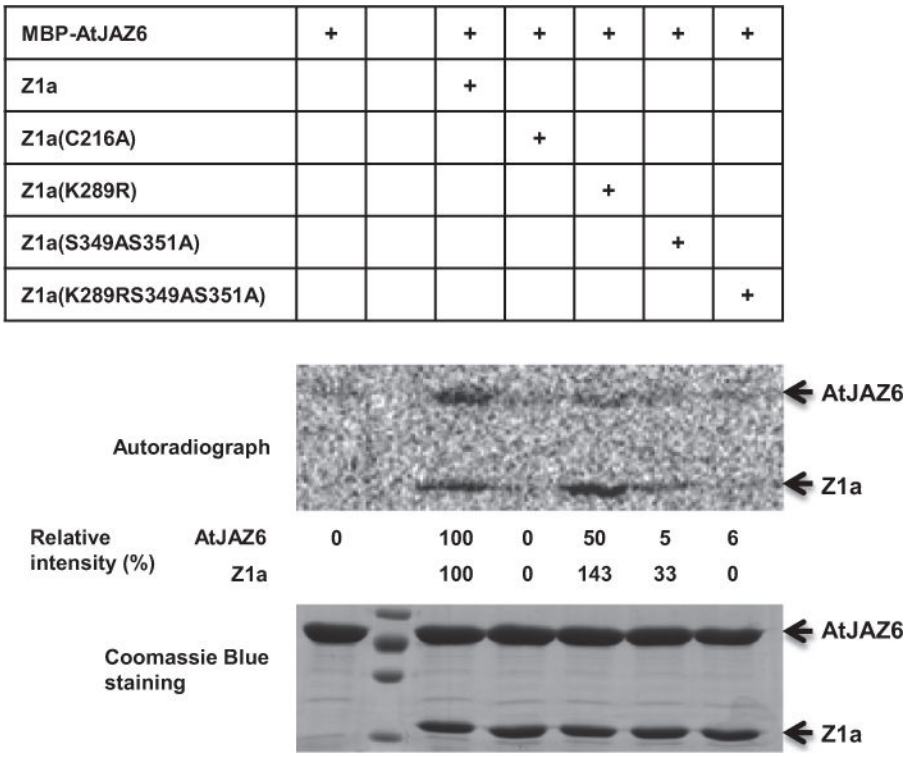

Fig. 2.

S349 and S351 are required for the acetyltransferase activity of HopZ1a. Tag-free proteins of wild-type and mutant HopZ1a were purified from *Escherichia coli* and examined for acetyltransferase activity using *in vitro* acetylation assays. MBP-AtJAZ6 was also purified from *E. coli* and used as a substrate. The reactions were supplemented with IP6. Numbers underneath the autoradiograph indicate relative levels of acetylation of AtJAZ6 by wild-type or mutant HopZ1a as well as the relative autoacetylation levels of HopZ1a. Equal loading of the proteins was confirmed by Coomassie Blue staining. These experiments were repeated three times with similar results.

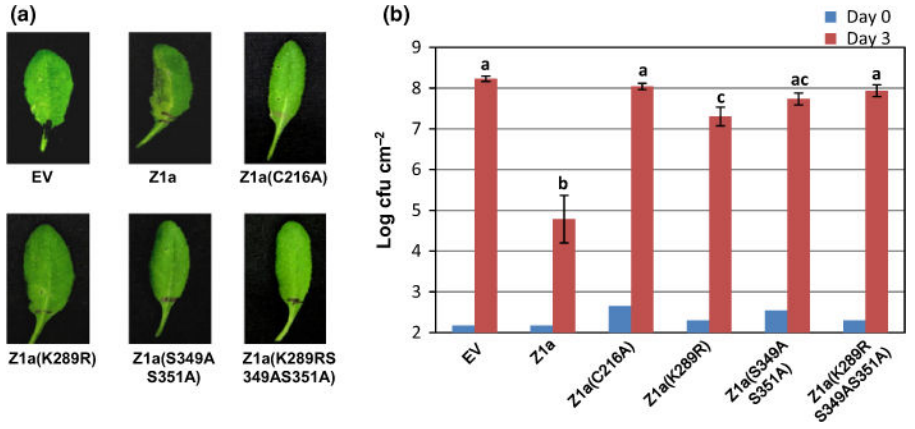

Fig. 3.

S349 and S351 are required for the hypersensitive response (HR)-triggering activity of HopZ1a in *Arabidopsis thaliana* ecotype Columbia (Col-0). (a) Substitutions of S349 and S351 abolished the cell death triggered by HopZ1a in *A. thaliana*. *Pseudomonas syringae* pv. *tomato* strain D28E (*Pto*D28E) expressing wild-type or mutant HopZ1a was infiltrated into leaves of 5-wk-old *A. thaliana* Col-0 plants at OD_{600} = 0.01 (1×10^7 cfu ml^{-1}). Cell death symptoms were monitored at 24 h post inoculation (hpi). *Pto*DC3000 carrying the empty vector pUCP20tk (EV) was used as a negative control. (b) Bacterial populations of *Pto*DC3000 expressing wild-type or mutant HopZ1a in *A. thaliana* Col-0. *Arabidopsis thaliana* leaves were infiltrated with *Pto*DC3000 carrying pUCP20tk (EV), or expressing wild-type or mutant HopZ1a at OD_{600} = 0.0001 (1×10^5 cfu ml^{-1}). Bacterial populations were determined at 0 and 3 d post inoculation. The average colony-forming units per square centimeter (cfu cm^{-2}) and ±SD (as error bars) are presented. Different letters at the top of the bars represent data for which differences were statistically significant (two-tailed *t*-test; $P < 0.05$). The expression of HopZ1a in *Pto*DC3000 was confirmed by western blots (Supporting Information Fig. S3). These experiments were repeated three times with similar results.

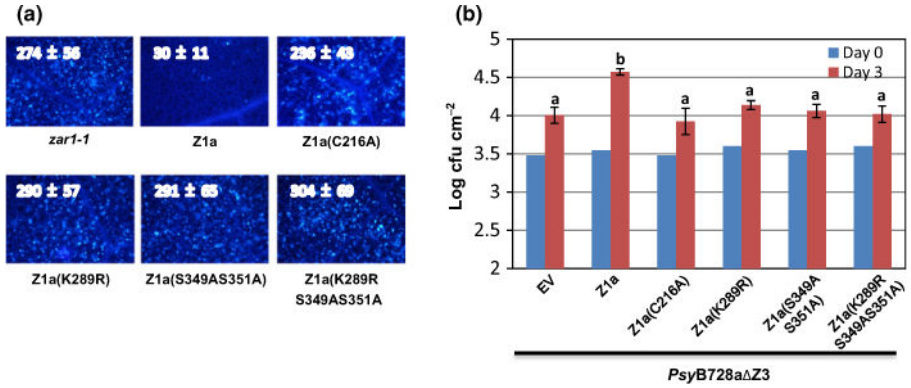

Fig. 4.

S349 and S351 are required for the virulence function of HopZ1a. (a) Mutations of S349 and S351 abolished the ability of HopZ1a to suppress flg22-mediated callose deposition. Adult leaves of 5-wk-old transgenic *Arabidopsis thaliana zar1-1* plants expressing wild-type or mutant HopZ1a were infiltrated with 1 μM flg22. The infiltrated leaves were collected at 16 h post infiltration and stained with aniline blue (MP Biomedicals, Santa Ana, CA, USA). Numbers of callose deposits in the infiltrated areas were numerated using fluorescent microscopy under UV. Values are mean ±SD (as error bars) (n = 12). (b) HopZ1a with S349 and S351 mutated can no longer promote the multiplication of *Pseudomonas syringae* pv. *syringae* strain B728aΔZ3 (*Psy*B728aΔZ3) in *Arabidopsis thaliana*. *Arabidopsis thaliana zar1-1* plants were infiltrated with *Psy*B728aΔZ3 carrying empty vector (EV), or expressing wild-type or mutant HopZ1a at OD_{600} = 0.005 (5×10^6 cfu ml^{-1}). Bacterial populations were determined at 0 and 3 d post inoculation. The average colony-forming units per square centimeter (cfu cm^{-2}) and ±SD (as error bars) are presented. Different letters at the top of the bars represent data for which differences were statistically significant (two-tailed t-test; $P < 0.05$). These experiments were repeated three times with similar results.

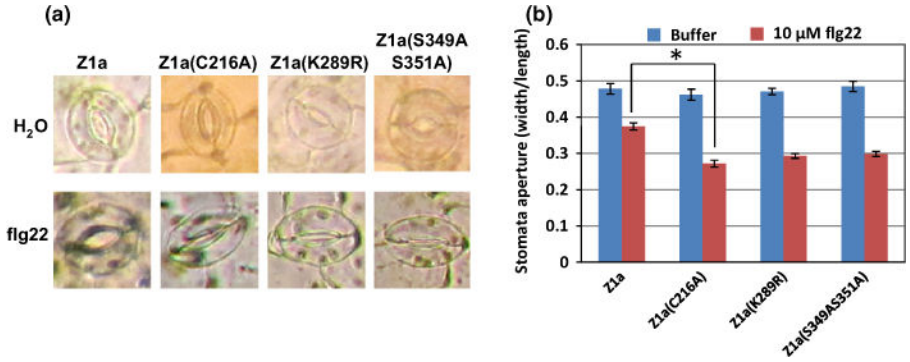

Fig. 5.

S349 and S351 are indispensable for HopZ1a to suppress stomatal defense. Leaf discs of 4-wk-old transgenic *Arabidopsis thaliana zar1-1* plants expressing wild-type or mutant HopZ1a were incubated with 10 μM flg22. Two hours after flg22 treatment, stomata on the lower epidermis were observed under a microscope. (a) Micrographs of stomata were used to measure the stomatal aperture, which is expressed as the ratio of width over length. (b) The average stomatal aperture and SE (as error bars). *Arabidopsis thaliana zar1-1* expressing HopZ1a(C216A) was used as a negative control. Data for which differences were statistically significant (two-tailed *t*-test): *, $P < 0.05$. The experiment was repeated twice with similar results.

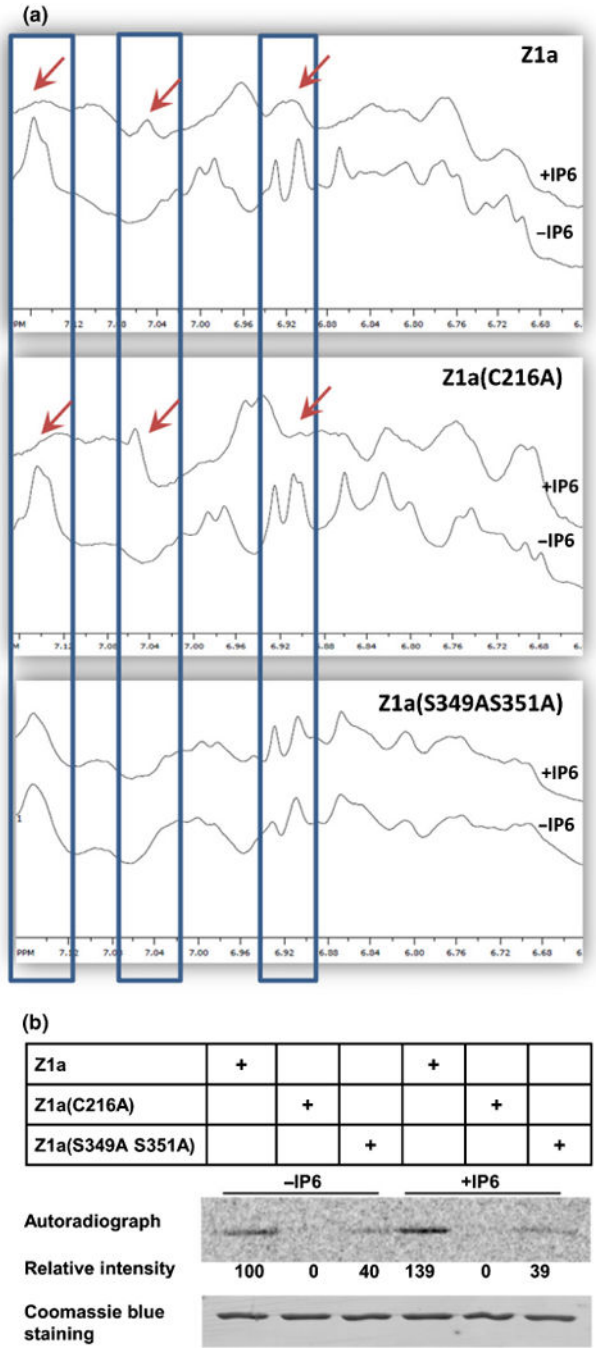

Fig. 6.

S349 and S351 affect the interaction of HopZ1a with inositol hexakisphosphate (IP6). (a) Analysis of the protein conformations of HopZ1a, HopZ1a(C216A) and HopZ1a(S349AS351A) in the presence or absence of IP6 by 1D ^{1}H nuclear magnetic resonance (NMR). Protein spectra of the aromatic region in the presence (upper traces) or absence (lower traces) of IP6 are shown. Spectral changes specifically induced by IP6 in HopZ1a and HopZ1a(C216A) are indicated by arrows. (b) *In vitro* acetylation assays of HopZ1a, HopZ1a(C216A) and HopZ1a(S349AS351A) in the presence or absence of IP6.

Numbers underneath the autoradiograph indicate relative acetylation levels of HopZ1a mutants compared with wild-type protein in the absence of IP6 (100%). Equal loading of the proteins was confirmed by Coomassie Blue staining. The experiment was repeated twice with similar results.

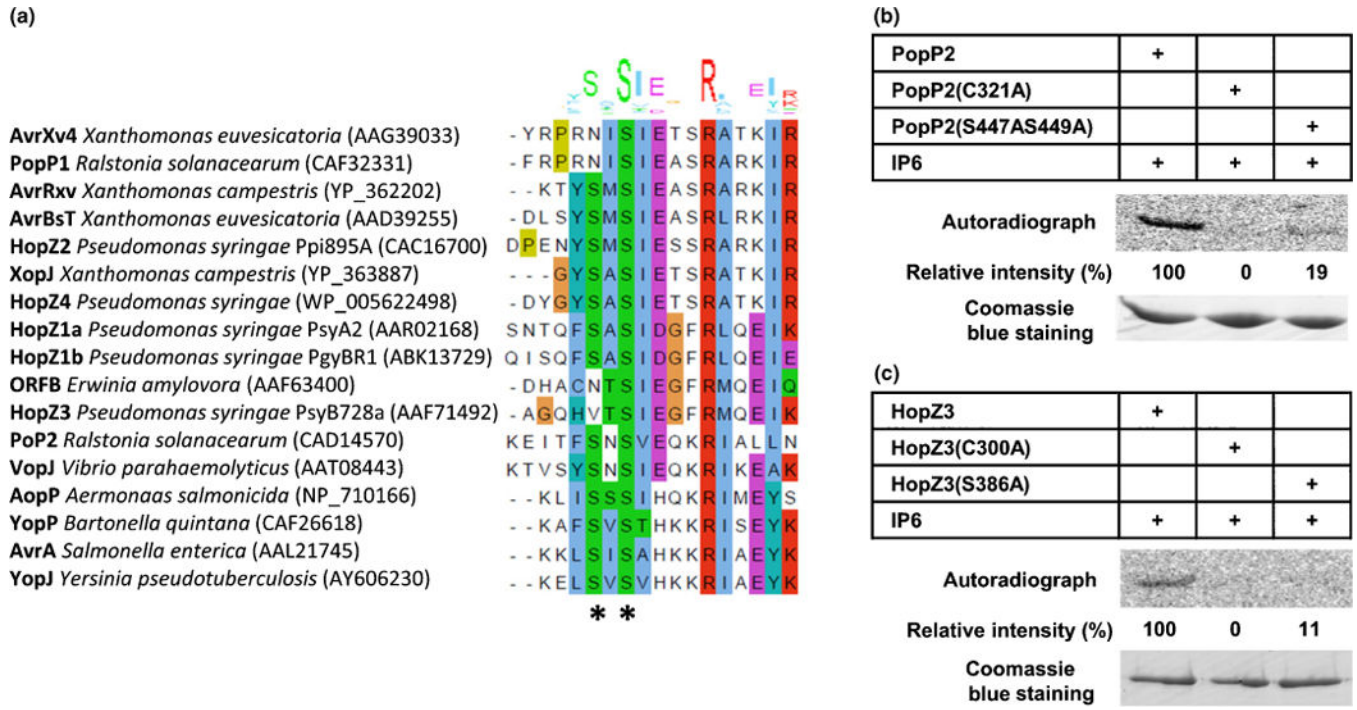

Fig. 7.

S349 and S351 have conserved functions in the YopJ family of acetyltransferases. (a) Amino acid sequence alignment in a conserved C-terminal region spanning residues 344–361 of HopZ1a and the corresponding region of other YopJ family effectors is shown. The accession numbers of each protein are presented in parentheses after the species name. Multiple sequence alignment was generated using $C_{LUSTAL}X$ (http://www.jalview.org/help/html/colourSchemes/clustal.html). A pictogram showing the relative frequency of amino acid occurrence at each position is presented above. S349 and S351 of HopZ1a are indicated by asterisks. A full-length amino acid sequence comparison is shown in Supporting Information Fig. S8. (b) *In vitro* acetylation assay of PopP2 produced by *Ralstonia solanacerum*. Tag-free PopP2, the catalytic mutant PopP2(C321A), and PopP2(S447AS449A) were purified from *Escherichia coli* and subjected to *in vitro* acetylation assay. (c) *In vitro* acetylation assay of HopZ3 produced by *Pseudomonas syringae* pv. *syringae*. HopZ3, the catalytic mutant HopZ3(C300A), and HopZ3(S386A) were purified from *E. coli* and subjected to *in vitro* acetylation assay. Numbers underneath the autoradiograph indicate relative acetylation levels of PopP2 or HopZ3 mutants compared with wild-type protein (100%). Equal loading of the proteins was confirmed by Coomassie Blue staining. These experiments were repeated three times with similar results.